Optimal Heck Cross-Coupling Catalysis: A Pseudo-Pharmaceutical Approach

Enrico Burello, Gadi Rothenberg*

Chemical Engineering Department, University of Amsterdam, Nieuwe Achtergracht 166, 1018 WV Amsterdam, The Netherlands
Fax: (+31)-20-525-5604, e-mail: gadi@science.uva.nl

Received: September 5, 2003; Accepted: October 31, 2003

Abstract: The problem of predicting the activity of ligands and solvents in homogeneous catalysis is addressed. A systematic selection method for ligands and solvents is presented, using a combination of stereoelectronic and electrotopological descriptors to describe the ligands and solvents in a set of 500 Heck reactions. Libraries of 'virtual ligands' and 'virtual solvents' are projected on the reaction space, and their reactivity is then predicted using multivariate models. The applications of this approach to combinatorial catalysis and reducing the amount of 'garbage data' are discussed.

Keywords: combinatorial catalysis; combinatorial chemistry; homogeneous catalysis; ligand optimisation; solvent optimisation

Introduction

The Heck reaction (palladium-catalysed coupling of aryl halides with alkenes) is one of the most useful protocols in organic synthesis.[1] It tolerates a wide range of conditions,[2] and its mechanism is reasonably well understood.[3–7] Nevertheless, it is still impossible to tell *a priori* what is the optimal ligand or the best solvent for a given Heck reaction. The variety of ligands is endless, and changing the solvent requires numerous tests and control experiments. Testing all combinations is not an option, even with robot synthesisers.[8,9] However, as we show here, it is possible to employ a screening approach similar to that used in drug design to preselect high-performance ligands and solvents for specific Heck reactions. The idea is to use multivariate techniques to construct a model that screens virtual libraries of ligands and solvents to find good candidates for future experiments.[10–12] To the best of our knowledge, this is the first example of applying pharmaceutical-type models to predict the activity of ligand and solvent libraries in homogeneous catalysis.[13–15]

To build robust predictive models for homogeneous catalysis, you must first assign quantitative descriptors to the various molecules in the system, and chose figures of merit for comparison. You can then train the model using a small set of well-defined reactions, and project the results on a library of catalysts. The most difficult part is deciding on the right descriptors.[16] The choice of figure of merit depends on the application. A 'good' catalyst is active, selective, and stable (for industrial purposes, cost is also a figure of merit). Here we use the turnover number (TON, denoted as $\mathbf{F}_1$) and the turnover frequency (TOF, denoted as $\mathbf{F}_2$). These are good indicators of activity and stability, and can be compared across the board as they are calculated per unit catalyst (TON) and per unit time (TOF).

Results and Discussion

Choosing and Calculating the Reaction Descriptors

In multivariate QSAR one defines the compound space using chemical descriptors (reaction-related) and molecular descriptors (structure-related). These variables may originate from experiments (empirical scales), or be calculated using quantum mechanical methods (e.g., HOMO/LUMO energies) or simply be based on atom/fragment counts. The descriptors must fulfil several requirements: They should be simple to calculate, they should be related to the figure(s) of merit, they should capture the structural variations within the data set, and, finally, they should be chemically meaningful. The last property is important, because it is the meaning of the descriptors that provides the link between the raw 'black' data and the chemists' intuitive explanation of this data (the 'white' model).

Often, it is difficult to know *a priori* the useful descriptors, so a reasonable starting point is to try to include as many descriptors as possible to account for the electronic and steric properties of molecules. Rank-reducing methods such as principal components analysis (PCA) can then reveal if and to what extent these descriptors are correlated with each other.

  DOI: 10.1002/adsc.200303141

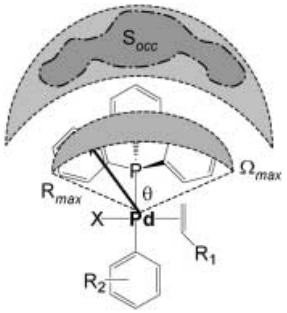

Scheme 1. Descriptors used to correlate stereoelectronic parameters of ligands. θ is Tolman's cone angle, R_{max} is the distance between the Pd atom and the bulkiest cross-section of the ligand, Ω_{max} is the solid angle at this cross-section, and S_{occ} is the percentage of the approach sphere occupied by the ligand.

Although we cannot know what the actual molecular structure of the active catalyst is, the effects of the ligand's structure and electronics are often the primary factors that determine the catalytic activity. Previous studies revealed that several parameters can be used to characterise steric and electronic properties of metal-coordinated compounds.[17] The most widely employed methods of estimating the steric requirements, for example, are Tolman's cone angle (Θ)[18] and the solid angle (Ω).[19,20] The Steric program[21] was used to determine Ω values and several other properties such as the radial profile, the area under its curve and the radius at its profile peak. All reagents, ligands and solvents were considered as 'ligands' with respect to the metal atom, so that the same set of stereoelectronic descriptors was employed for all the compounds that bind to the metal. We found that good correlations could be obtained, for the ligand sterics using just two parameters: the distance between the metal atom and the bulk of the ligand, R_{max}, and the solid angle that pertains to this distance, Ω (Scheme 1).[22]

In addition, many other descriptors that reflect structural properties such as the molecular weight, the van der Waals surface, and the volume of molecules were computed. The electronic properties of molecules were characterised using the atomic charges of the ligating P atoms (for ligands only), the HOMO and LUMO energies, the dipole moments and the molecular polarisabilities. Solvent effects were further quantified by introducing an additional set of several empirical and theoretical descriptors (see Table 2 for a complete list).

We then collected from the literature experimental data for 500 Heck reactions that were performed using different reagents, solvents and ligands.[23–35] The data were set up as a matrix **X** wherein each row represents one reaction, and the columns represent the *x* and *y* variables (respectively the 80 descriptors and the two figures of merit). Table 1 shows a partial representation of the dataset. Multivariate quantitative structure-activity relationship (MQSAR) models[10] were then

Table 1. Partial representation of the 500 × 82 reaction dataset.[a]

Entry	Reaction conditions[b]					Molecular descriptors[c]				Figures of merit	
	Aryl halide X/R_1	Alkene R_2	Ligand	Solvent	T [°C]	Volume [Å^3]		Dipole moment [Debye]		F_1 (TON) × 10^3	F_2 (TOF) × 10^3
						Ligand	Solvent	Ligand	Solvent		
1	Br/*p*-OH	Styrene	P(*o*-tol)$_3$	NEt_3	100	307	93.1	0.095	0.72	44.0	0.102
2	Br/*p*-OH	Styrene	P(*o*-tol)$_3$	NEt_3	100	307	93.1	0.095	0.72	76.0	0.4
3	Cl/H	CO_2*n*-Me	P(*t*-Bu)$_3$	NMP	100	238	96.6	1.109	3.75	93.3	0.116
4	Br/*p*-OH	CO_2Me	P(*o*-tol)$_3$	NEt_3	75	307	140	0.095	0.72	44.0	2.00
5	I/*o*-OH	CO_2Me	PPh_3	NEt_3	100	258	140	0.712	0.72	83.0	9.20
6	Br/*o*-Me	CO_2Me	P(*t*-Bu)$_3$	Dioxane	25	238	85.7	1.109	0.46	19.4	1.16
7	Br/*o*-Me	CO_2Me	P(*t*-Bu)$_3$	Dioxane	25	238	85.7	1.109	0.46	34.0	4.25
8	I/H	Styrene	P(OPh)$_3$	DMF	80	286	77.4	2.27	3.79	8	1.71
9	I/H	Styrene	P(*o*-tol)$_3$	DMF	80	307	77.4	0.095	3.79	12	2.66
10	I/H	Styrene	PPh_3	DMF	80	258	77.4	0.712	3.79	6	1.33
11	Br/*p*-OH	CO_2Et	P(*o*-tol)$_3$	DMF	130	307	77.4	0.095	3.79	12.0	0.50
12	Cl/*o*-Me	Ph	P(*t*-Bu)$_3$	Dioxane	120	238	85.7	1.109	0.46	35.0	0.30
13	Br/*p*-OH	CO_2Me	PPh_3	NEt_3	75	258	140	0.712	0.72	3.0	0.50
14	Br/*p*-OH	CO_2Me	P(*o*-tol)$_3$	NEt_3	75	307	140	0.095	0.72	95.0	1.94
15	Br/*p*-OH	CO_2Me	P(*p*-tol)$_3$	NEt_3	80	309	140	0.908	0.72	26.0	0.58

[a] Each row represents a different reaction characterised by the aryl halide, the alkene, the ligand and the solvent.
[b] A basic assumption in QSAR analysis is that the dataset is homogeneous. Because of this, we limited our data to the substrates as follows: Ligands were either mono- or bi-phosphines, and only ten dipolar aprotic solvents were included: DMA, DMF, THF, 1,2-DCE, Et_3N, PhMe, MeCN, HMPA, NMP, and dioxane.
[c] Thirty-three steric and electronic descriptors were calculated (see Table 2 for a complete list).

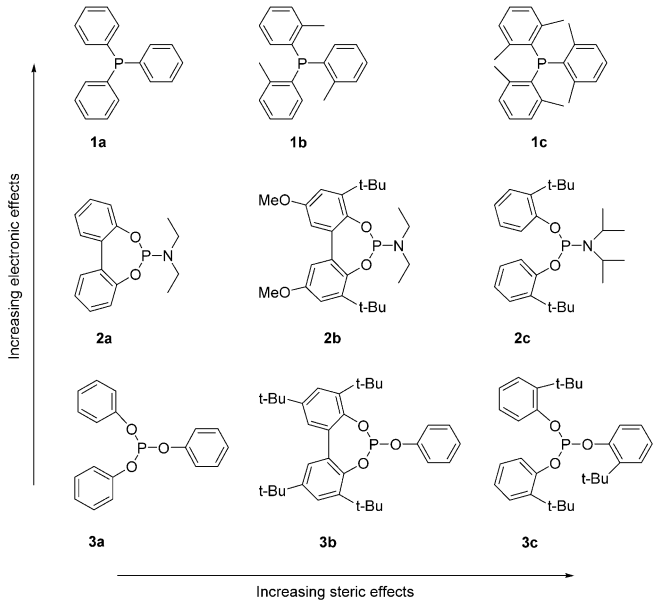

Scheme 2. Ligands tested by van Strijdonck et al. in the Heck reaction between styrene and iodobenzene in MeCN at 80 °C. These nine ligands are used as a training set for the *in silico* ligand design experiment shown in Figure 1.

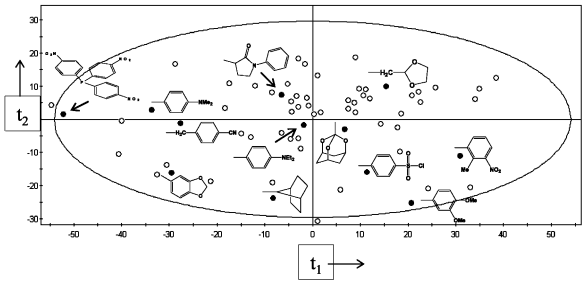

Figure 1. Projection of a virtual ligand library on the ligands space. The '●' symbols represent PR_3 ligands with R structures as shown [for example, the full structure for $P(C_6H_4NO_2)_3$ is given on the left] were selected by the model as the 12 best candidates, using the training set shown in Scheme 2.

used to screen virtual libraries of ligands and solvents. A principal component analysis (PCA) showed that the 500 reactions divide into eight clusters of 50 – 100 reactions each, with each cluster reflecting the different catalytic conditions applied. Here the term "cluster" corresponds to a set of data in which several classes of reactions are encountered. Reactions in a cluster display similar descriptor values. A cluster can be defined by measuring the (small) distance between intra-cluster observations and the larger distance/diversity between two reactions belonging to two different clusters. In our case, reactions that were performed using ligands and solvents with the same structural and electronic characteristics under similar conditions (T, t, Ligand : Pd ratios, etc.) were assigned to the same cluster.

Due to the incomplete nature of the dataset, we could not build a single unified model. Instead, independent models to optimise ligands and solvents were constructed for each cluster.

Ligand Optimisation

Ligand design is considered almost an art in homogeneous catalysis.[36] Small variations in the ligand structure can cause large differences in catalytic performance.[37] As an example, we considered the case for PR_3 ligands. The number and type of moieties bound to the ligating phosphorus atom and the substituents on these have a strong influence on the catalyst's activity. To quantify these effects a further QSAR analysis was performed, now including topological and structural descriptors to characterise also the elemental composition and the molecular connectivity of the ligand. On every subset of reactions that yielded a good partial least squares (PLS) model, we could now project a library of 'virtual ligands'.

This approach is best demonstrated by way of example: Let us consider the experiments of van Strijdonck et al.,[33] who tested a set of nine ligands for the Heck coupling of styrene with iodobenzene (Scheme 2). Using these data as a training set, we screen *in silico* a virtual library of seventy PR_3 ligands assembled from commercially available precursors.[38] We calculate the descriptors for these ligands and then backtrack using the PLS model to predict their corresponding TON and TOF values in the same Heck system. Figure 1 shows the analysis results. '○' symbols represent the entire ligand library and '●' symbols indicate the twelve most promising potential ligands, together with their molecular structures. These twelve ligands are predicted to give high TON and TOF values in the above Heck reaction. Note also that the selected compounds show a wide structural diversity – ligands with different structures can indeed have high figures of merit in the same reaction.

The advantage of this method is that you do not have to test all the permutations – the model gives you an indication where to search in the ligand space. The disadvantage is that for reliable predictions you must have a good experimental training set, which may not be easy to obtain.

Solvent Optimisation

The solvents usually employed in Heck reactions are dipolar aprotic σ-donors. However, most studies cover only a small number of solvents, partly because this means a large increase in the number of experiments and controls. Our approach to solvent optimisation was similar to the ligand tests described above: First, we

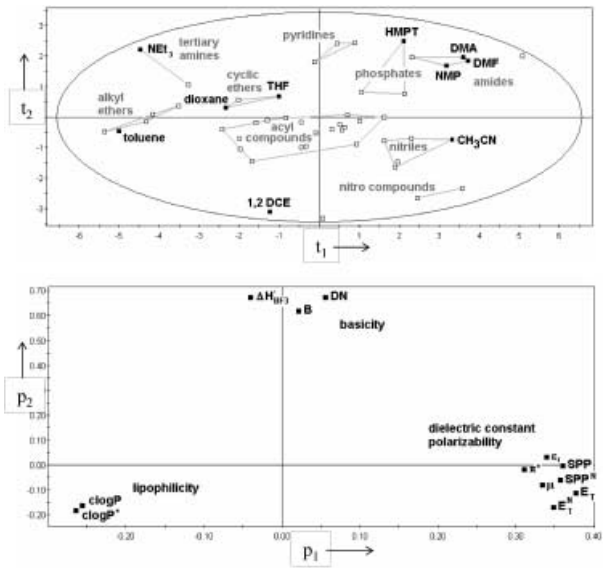

Figure 2. Solvent 'constellations' (top) mapped according to the correlation between the solvent descriptors (bottom). The abscissa p_1 reflects the degree of solvent/solute likeness (lipophilic/polar) and the ordinate p_2 the degree of donicity – the coordination ability of the solvent.[46]

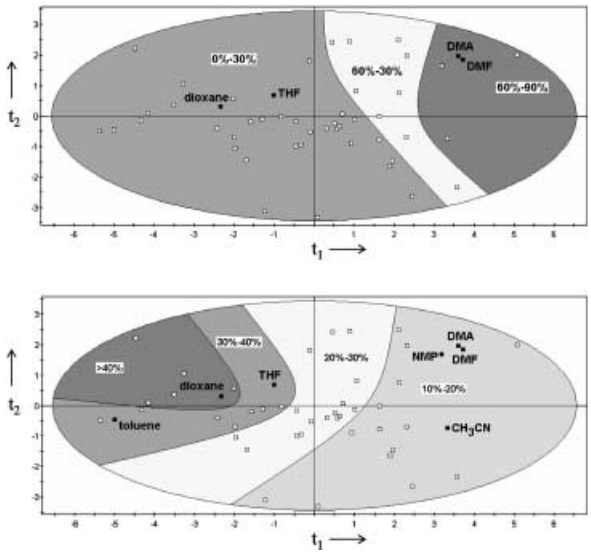

Figure 3. Two examples showing the application of the solvent map to preselect solvents for Heck reactions. Black squares show solvents that were used in the experimental reactions, while white squares show virtual solvents projected on the experimental data.

assigned a set of empirical and theoretical scales for solvent characterization.[39] Then, we used these scales to characterise fifty solvents, only ten of which are normally used in the Heck reaction. A PCA analysis on the resulting dataset showed that the scales are correlated and well described by the first two components t_1 and t_2 that reflect the solvents' polarity and basicity, respectively ($R^2X_{cum} = 0.864$ and $Q^2_{cum} = 0.731$,[40] see Figure 2, top). This characterisation is in good agreement with the unified scales found by Drago and co-workers.[41,42] This analysis gives a solvent chart, similar to a star chart, (Figure 2, bottom) in which the various classes of solvents are shown as 'solvent constellations'.

With prior knowledge on solvent performance you can use PLS analysis to determine which areas in the PCA score plot are worth sampling. This means that if you carry out Heck reactions in a few solvents, you can use the model to define areas in the solvent chart where high yields are likely. Again, it is easiest to give an example: Figure 3 shows two cases based on data of Nolan and co-workers[34] and Littke and Fu.[26] The former used THF, dioxane, DMF, and DMA. The latter tested THF, dioxane, DMF, DMA, NMP, toluene, and MeCN (all these solvents are shown as black squares). In both cases, and this is crucial for the comparison, all other parameters except the solvent were kept constant. Note the differences between Figure 3 top and bottom: In the first case, increasing the solvent polarity clearly enhances the product yield, while in the second case higher yields are afforded using solvents that are both basic and polar.

As in the case for ligands, it is possible to project the experimental results on the solvent chart and to preselect solvents that may perform well in the reaction. Figure 3 also shows the positions of fifty other solvents (not tested in these Heck reactions, shown as white squares). The optimal solution is not always obvious. For example, alkyl ethers and tertiary amines (cf. Figures 3 and 2) are predicted as better solvents, in the case of the experiments of Littke and Fu, than the well known DMF, DMA, and NMP.

Most homogeneous reactions are performed in dilute solutions, so we may assume that the solvents' properties are not influenced by the reaction itself. This is important, because it means that the 'solvent constellations' shown in Figure 2 are static – they need be calculated only once. Moreover, the solvent descriptors in Figure 2 are orthogonal and give good PLS results ($Q^2 > 0.91$) for several models. This means that the solvent map is not necessarily limited to the reaction clusters studied above, but may find use also as a general selection tool in homogeneous catalysis.

Finally, it is worthwhile to consider other types of clusters in the data. The (halide) leaving group on the aromatic ring is considered important for two reasons: First, because the rate-determining step changes when you move from iodide to chloride ($I > Br >> Cl$), and second because the halide counter anion may affect the catalytic properties. To test for these effects, we also made sub-clusters of the reactions according to the type of halide and treated each group separately. More variance was explained by these models, but the disadvantage is that they pertain to smaller groups of

Table 2. Molecular descriptors and empirical scales.

Entry	Symbol	Description
Electronic descriptors[a]		
1	σ_m	Hammett constant, *meta* position
2	σ_p	Hammett constant, *para* position
3	E_{HOMO}	Highest Occupied Molecular Orbital energy
4	E_{LUMO}	Lowest Unoccupied Molecular Orbital energy
5	GAP	$E_{LUMO} - E_{HOMO}$
6	μ	Dipole moment
7	$q_{1,P}$	Electrostatic potential on P atom
8	$q_{2,P}$	Mulliken charge on P atom
Steric descriptors[b]		
9	Mw	Molecular weight
10	Surface	Van der Waals surface
11	Volume	Volume enclosed in van der Waals surface
12	Θ	Tolman's cone angle
13	Ω	Solid angle
14	Ω_{max}	Maximum numerical solid angle
15	S_{occ}	Percentage of sphere occupation
16	A_{sap}	Area under numerical solid angle profile
17	R_{max}	Radius at numerical solid angle profile peak
Empirical scales[c]		
18	n	Refractive index
19	ε_r	Dielectric constant
20	d^{25}	Density at 25 °C
21	ΔH	Standard molar enthalpy of vaporization
22	ΔU	Standard internal energy of vaporization
23	Δ_H	Cohesive energy density
24	AN	Solvent acceptor number
25	DN	Solvent donor number
26	π^*	Polarisability
27	E_T	Electronic transition energy of pyridinium *N*-phenolate betaine dye
28	E_T^N	Electronic transition energy of pyridinium N-Phenolate betaine dye (normalized)
29	B	Basicity from stretching frequency of CH_3OD in different solvents
30	$\Delta H^\circ_{BF_3}$	Enthalpy of complexation of solvents with BF_3 in dichloromethane
31	SPP^N	UV/vis spectra of 2-dimethylamino-7-nitrofluorene and 2-fluoro-7-nitrofluorene
32	SPP	Solvatochromic shifts of long wavelength absorption maximum of 2-(dimethylamino)-7-nitrofluorene and 2-fluoro-7-nitrofluorene
33	ClogP	$^{Octanol}/_{water}$ partition coefficient (sum of fragment contributions)[d]

[a] Electronic descriptors were calculated for ligands, solvents and reagents R_1 and R_2 except for Hammett constants (σ_m and σ_p) and the P atom charges ($q_{1,P}$ and $q_{2,P}$) used to characterise respectively electronic properties of aryl halides and ligands.
[b] Steric descriptors were calculated for all the compounds.
[c] Empirical scales were used to characterise only solvent properties.
[d] The ClogP program is available free online at http://www.daylight.com/daycgi/clogp.

reactions. The development of descriptors to study counter-ion effects will be the subject of future research in our laboratory.

Conclusions

By choosing the appropriate descriptors one can correlate the structural and chemical variation in a large set of catalytic reactions. We are still working on a unified model, but cluster analysis already gives good results ($Q^2_{cum} > 0.7$). Even considering the uneven nature of the data and the incompleteness of the set, quantitative models can be used to preselect good reaction conditions. Moreover, it is possible to superimpose 'virtual ligands' and 'virtual solvents' on the dataset by assigning their descriptors and then backtracking to predict their catalytic performance. In this way, the number of redundant experiments and the amount of 'garbage data' (and the cost associated with these) can be significantly reduced. We believe that this approach, when combined with the speed and reproducibility of modern high-throughput experimental systems,[43] could eventually enable chemists to reproduce the pharma-

ceutical success of combinatorial chemistry in homogeneous catalysis.

Experimental Section

Computational Methods

The dataset matrix **X** is composed of 500 observations (the Heck reactions) and 80 variables (we used approximately 20 descriptors for each molecule type). In multivariate QSAR, principal component analysis (PCA) is a useful technique to display observations and identify redundant information among the variables. PCA finds a limited number of new variables, **t**, called the principal component scores, that summarise the information in the original variables. Mathematically, PCA corresponds to a factorisation of the **X** matrix as the product of the smaller matrices, **T** and **P**′, comprised of the compound scores and the variable loadings, respectively. In matrix notation this is:

$$X = \mathbf{1} \cdot \bar{x} + T \cdot P' + E \quad (1)$$

where **1** denotes a column vector of ones, $\bar{x}$ is a row vector containing the variable averages, and **E** is a matrix of residuals. The principal component scores, **T**, express the relationship between the compounds. The variable loadings, **P**′, display the relationships among the variables. We assumed no prior knowledge about the variables' importance and gave all of the descriptors equal importance by autoscaling them to unit variance.

To obtain a predictive model that relates the descriptors to the output measurements (the figures of merit TON and TOF) we performed a partial least squares (PLS) analysis. PLS works with two matrices, **X** and **Y**, the former containing the descriptors and the latter the figures of merit. PLS is used to approximate **X** and **Y** and to model the relationship between them. The PLS regression model can be expressed as:

$$Y = X \cdot B_{PLS} + F \quad (2)$$

where $\mathbf{B}_{\mathrm{PLS}}$ corresponds to regression coefficients determined from the underlying latent variable model, and **F** to the unmodeled residuals. The regression coefficients can be used for assessing which *x*-variables mainly model a certain *y*-variable. However, with correlated variables, these coefficients are not mathematically independent. PLS estimates the correlation structure between **X** and **Y** in terms of projections onto a few latent variables. The resulting PLS *x*-weight vectors are used to combine the *x*-variables with the scores, **t**, that predict the *y*-variables.

The statistical performance of a PLS model is deduced from the statistics R^2Y (explained *y*-variation) and Q^2 (predicted *y*-variation). The former quantity is calculated as $1 - \mathrm{RSS}/\mathrm{SS}_\gamma$, where RSS is the residual sum of squares of the response data and SS_γ the response sum of squares (corrected for the mean). In a similar fashion, Q^2 is computed as $1 - \mathrm{PRESS}/\mathrm{SS}_\gamma$, where PRESS is the predictive residual sum of squares of the response data. The explained variation, R^2, varies between 0 and 1.

Internal validation of the models was performed using cross-validation (CV). Here, observations are kept out of the model development, then the figures of merit for these observations are predicted by the model and compared with the actual values. This procedure is repeated several times until every observation has been kept out once (and only once). The prediction error sum of squares [PRESS, Eq. (3)] is the squared differences between observed y^{obs} and predicted values y^{pred} when the observations were kept out, and SS is the residual sum of squares of the previous dimension [Eq. (4)]. The value Q = PRESS/SS is then computed for every dimension, and a component is considered significant if $Q < 1$.

$$PRESS = \sum_i \sum_j \left(y_{ij}^{obs} - x_{ij}^{pred}\right)^2 \quad (3)$$

$$SS = \sum_i \sum_j \left(y_{ij}^{obs} - y_{ij}^{mean}\right)^2 \quad (4)$$

Table 2 gives a full list of the descriptors used in this study. Note that it is important to choose an efficient method of calculation to establish equilibrium geometries of molecules. Among the quantum-based methods which are least CPU costly we chose the PM3 semi-empirical method[44] within the Spartan[45] package program.

References and Notes

[1] I. P. Beletskaya, A. V. Cheprakov, *Chem. Rev.* **2000**, *100*, 3009.
[2] J. G. de Vries, *Can. J. Chem.* **2001**, *79*, 1086.
[3] A. F. Shmidt, V. V. Smirnov, O. V. Starikova, A. V. Elaev, *Kinet. Catal.* **2001**, *42*, 199.
[4] G. T. Crisp, *Chem. Soc. Rev.* **1998**, *27*, 427.
[5] M. Casey, J. Lawless, C. Shirran, *Polyhedron* **2000**, *19*, 517.
[6] C. Amatore, E. Carre, A. Jutand, M. A. M'Barki, G. Meyer, *Organometallics* **1995**, *14*, 5605.
[7] C. Amatore, M. Azzabi, A. Jutand, *J. Am. Chem. Soc.* **1991**, *113*, 8375.
[8] G. Rothenberg, H. F. M. Boelens, D. Iron, J. A. Westerhuis, *Catalysis Today* **2003**, *81*, 359.
[9] G. Rothenberg, H. F. M. Boelens, D. Iron, J. A. Westerhuis, *Chim. Oggi* **2003**, *21*, 80.
[10] L. Eriksson, E. Johansson, *Chemom. Intell. Lab. Sys.* **1996**, *34*, 1.
[11] M. Karelson, V. S. Lobanov, A. R. Katritzky, *Chem. Rev.* **1996**, *96*, 1027.
[12] G. R. Famini, L. Y. Wilson, *J. Phys. Org. Chem.* **1999**, *12*, 645.
[13] I. Muegge, S. L. Heald, D. Brittelli, *J. Med. Chem.* **2001**, *44*, 1841.
[14] M. W. Lutz, J. A. Menius, T. D. Choi, R. G. Laskody, P. L. Domanico, A. S. Goetz, D. L. Saussy, *Drug Discov. Today* **1996**, *1*, 277.
[15] K. D. Cooney, T. R. Cundari, N. W. Hoffman, K. A. Pittard, M. D. Temple, Y. Zhao, *J. Am. Chem. Soc.* **2003**, *125*, 4318.
[16] L. Perrin, E. Clot, O. Eisenstein, J. Loch, R. H. Crabtree, *Inorg. Chem.* **2001**, *40*, 5806.
[17] T. L. Brown, K. J. Lee, *Coord. Chem. Rev.* **1993**, *128*, 89.

[18] C. A. Tolman, *Chem. Rev.* **1976**, #76#77, 313.
[19] D. White, B. C. Tavener, P. G. L. Leach, N. J. Coville, *J. Organomet. Chem.* **1994**, *478*, 205.
[20] D. White, B. C. Taverner, P. G. L. Leach, N. J. Coville, *J. Comput. Chem.* **1993**, *14*, 1042.
[21] Copyright 1994,1995 C. T. Steric, All rights reserved.
[22] J. M. Smith, B. C. Taverner, N. J. Coville, *J. Organomet. Chem.* **1997**, *530*, 131.
[23] I. P. Beletskaya, A. N. Kashin, N. B. Karlstedt, A. V. Mitin, A. V. Cheprakov, G. M. Kazankov, *J. Organomet. Chem.* **2001**, *629*, 219.
[24] C. B. Ziegler, R. F. Heck, *J. Org. Chem.* **1978**, *43*, 2941.
[25] W. A. Herrmann, C. Brossmer, K. Ofele, M. Beller, H. Fischer, *J. Mol. Catal. A: Chem.* **1995**, *103*, 133.
[26] A. F. Littke, G. C. Fu, *J. Org. Chem.* **1999**, *64*, 10.
[27] A. F. Littke, G. C. Fu, *J. Am. Chem. Soc.* **2001**, *123*, 6989.
[28] A. M. Magill, D. S. McGuinness, K. J. Cavell, G. J. P. Britovsek, V. C. Gibson, A. J. P. White, D. J. Williams, A. H. White, B. W. Skelton, *J. Organomet. Chem.* **2001**, *617*, 546.
[29] F. Miyazaki, K. Yamaguchi, M. Shibasaki, *Tetrahedron Lett.* **1999**, *40*, 7379.
[30] A. Spencer, *J. Organomet. Chem.* **1984**, *270*, 115.
[31] A. Spencer, *J. Organomet. Chem.* **1983**, *258*, 101.
[32] J. P. Stambuli, S. R. Stauffer, K. H. Shaughnessy, J. F. Hartwig, *J. Am. Chem. Soc.* **2001**, *123*, 2677.
[33] G. P. F. van Strijdonck, M. D. K. Boele, P. C. J. Kamer, J. G. de Vries, P. W. N. M. van Leeuwen, *Eur. J. Inorg. Chem.* **1999**, 1073.
[34] C. L. Yang, H. M. Lee, S. P. Nolan, *Org. Lett.* **2001**, *3*, 1511.
[35] K. H. Shaughnessy, P. Kim, J. F. Hartwig, *J. Am. Chem. Soc.* **1999**, *121*, 2123.
[36] C. Masters, *Homogeneous transition-metal catalysis – a gentle art*, Chapman & Hall, London, **1981**.
[37] M. M. Rahman, H. Y. Liu, K. Eriks, A. Prock, W. P. Giering, *Organometallics* **1989**, *8*, 1.
[38] The total number of ligands in this virtual library is 54,740, but we limited the set to the seventy simple symmetric compounds.
[39] A. R. Katritzky, T. Tamm, Y. L. Wang, M. Karelson, *J. Chem. Inf. Comput. Sci.* **1999**, *39*, 692.
[40] Q^2 is the fraction of the total variation of the X's (descriptors) that can be predicted by a principal component t while Q^2_{cum} is the sum of Q^2 over all the principal components. R^2X is the fraction of the Sum of Squares of all the X's explained by a principal component t while R^2X_{cum} is the cumulative SS of all the X's explained by all extracted components.
[41] L. Mu, R. S. Drago, D. E. Richardson, *J. Chem. Soc. Perkin Trans. 2* **1998**, 159.
[42] R. S. Drago, M. S. Hirsch, D. C. Ferris, C. W. Chronister, *J. Chem. Soc. Perkin Trans. 2* **1994**, 219.
[43] H. F. M. Boelens, D. Iron, J. A. Westerhuis, G. Rothenberg, *Chem. Eur. J.* **2003**, *9*, 3876.
[44] N. T. Anh, G. Frison, A. Solladie-Cavallo, P. Metzner, *Tetrahedron* **1998**, *54*, 12841.
[45] Spartan is distributed by Wavefunction Inc., 18401 Von Karman Ave., #370, Irvine, CA 92612 USA, © Wavefunction Inc.
[46] The PC analysis provides values of the so-called loading vectors **p**, showing how the descriptors are combined to form the scores **t**. A plot of the loading vectors indicates which of the descriptors are important, and corresponds to the directions in the score plot. The $\mathbf{p}_1$ *vs.* $\mathbf{p}_2$ plot shows the importance of the descriptors in the approximation of the data set matrix **X**. The position of an observation (a reaction) in a given direction of the score plot $\mathbf{t}_1/\mathbf{t}_2$ is influenced by the descriptors lying in the same direction in the loading $\mathbf{p}_1/\mathbf{p}_2$ plot.

